

# The Hu-Zhang element for linear elasticity on curved domains

Wei Chen · Xinyuan Du · Jun Hu

Received: date / Accepted: date

**Abstract** This paper extends the Hu-Zhang element for linear elasticity problems to curved domains, preserving strong symmetry and  $H(\text{div})$ -conformity. The non-polynomial structure of the curved Hu-Zhang element makes it difficult to analyze the stability result, which is overcome by establishing a novel inf-sup condition. Optimal convergence rates are achieved for all variables except the stress  $L^2$ -error. This suboptimality originates from the fact that the divergence space of the curved Hu-Zhang element is not contained in the discrete displacement space, which is rectified by local  $p$ -enrichment in the Hu-Zhang space on curved boundary elements. Some numerical experiments validate the theoretical results.

**Keywords** Linear elasticity problems · Symmetric stress tensor · Parametric finite elements · Inf-sup condition · Convergence analysis

**Mathematics Subject Classification (2020)** 65N12 · 65N30 · 74S05

---

The third author was supported by the National Natural Science Foundation of China Grants No. NSFC 12288101.

---

Wei Chen

LMAM and School of Mathematical Sciences, Peking University, Beijing 100871, P. R. China  
Chongqing Research Institute of Big Data, Chongqing 401329, P. R. China  
E-mail: 2406397052@pku.edu.cn

Xinyuan Du

LMAM and School of Mathematical Sciences, Peking University, Beijing 100871, P. R. China  
E-mail: 2301110045@stu.pku.edu.cn

Jun Hu

LMAM and School of Mathematical Sciences, Peking University, Beijing 100871, P. R. China  
Chongqing Research Institute of Big Data, Chongqing 401329, P. R. China  
E-mail: hujun@math.pku.edu.cn

## 1 Introduction

Let  $\Omega \subset \mathbb{R}^2$  be a bounded connected domain with piecewise  $C^{r+1}$  boundary  $\Gamma$ . Given a load  $f \in L^2(\Omega; \mathbb{R}^2)$ , consider the Hellinger-Reissner formulation for the linear elasticity problem with homogeneous displacement boundary conditions: find  $(\sigma, u) \in \Sigma \times V := H(\operatorname{div}, \Omega; \mathbb{S}) \times L^2(\Omega; \mathbb{R}^2)$ , such that

$$\begin{cases} a(\sigma, \tau) + b(\tau, u) = 0, & \text{for all } \tau \in \Sigma, \\ b(\sigma, v) = -(f, v), & \text{for all } v \in V, \end{cases} \quad (1)$$

where the bilinear forms are defined by

$$a(\sigma, \tau) := (\mathcal{A}\sigma, \tau), \quad b(\tau, v) := (\operatorname{div} \tau, v), \quad (2)$$

and  $\mathbb{S}$  denotes the space of symmetric tensors of  $\mathbb{R}^{2 \times 2}$ . The compliance tensor  $\mathcal{A} = \mathcal{A}(x) : \mathbb{S} \rightarrow \mathbb{S}$ , characterizing material elastic properties, is bounded and symmetric positive definite uniformly for  $x \in \Omega$ . For isotropic materials,  $\mathcal{A}$  takes the form:

$$\mathcal{A}\sigma := \frac{1}{2\mu} \left( \sigma - \frac{\lambda}{2\lambda + 2\mu} (\operatorname{tr} \sigma) \mathbf{I} \right). \quad (3)$$

Here  $\mathbf{I}$  is the  $2 \times 2$  identity matrix,  $\operatorname{tr}(\cdot)$  denotes the trace operator. The Lamé constants  $\lambda$  and  $\mu$  are positive material parameters.

Constructing stable mixed finite element spaces for the Hellinger-Reissner formulation (1) is a longstanding challenge due to the requirement of symmetric stress fields [9, 10]. Early developments in this direction include composite elements and weakly symmetric approaches [2, 5, 6, 40, 43, 52, 53]. In [9], Arnold and Winther designed the first family of mixed finite element methods in two dimensions, based on polynomial shape function spaces. From then on, various stable mixed elements have been constructed, see e.g., [1, 3, 4, 7, 9–11, 16, 24, 26, 30–32, 35, 36, 42, 57, 58]. Recently, Hu [33] proposed a family of conforming mixed elements on simplicial meshes for any dimension, with specific implementations in 2D [37] and 3D [38]. This new class of elements requires fewer degrees of freedom than those in the earlier literature. For  $k \geq n + 1$ , the stress tensor is discretized by  $P_k$  finite element subspace of  $H(\operatorname{div})$  and the displacement by piecewise  $P_{k-1}$  polynomials. Moreover, a new idea is proposed to analyze the discrete inf-sup condition, and the basis functions therein are easy to obtain. For the case that  $1 \leq k \leq n$ , the symmetric tensor space is enriched by proper high-order  $H(\operatorname{div})$  bubble functions to stabilize the discretization in [39]. Another method by stabilization technique to deal with this case can be found in [22, 23, 55]. Corresponding mixed elements on both rectangular and cuboid meshes are constructed in [34].

In practical engineering analyses of curved domains, the geometric consistency error induced by polygonal boundary approximations fundamentally limits the convergence rates of finite element methods. For second-order elliptic equations discretized with  $k$ -th order standard finite element methods on meshes of geometric approximation order  $m$ , the  $H^1$ -error between the numerical and exact solutions is dominated by two key contributions: the geometric

consistency error  $\mathcal{O}(h^m)$  and the polynomial approximation error  $\mathcal{O}(h^k)$ . Rigorous proofs of this error estimate can be found in [13, 25, 41, 46]. To guarantee optimal convergence rates,  $m$  must equal or exceed  $k$  (isoparametric or superparametric approximation). Although standard curved finite element methods are mature [19–21, 51], the application of mixed formulation to linear elasticity problems on curved domains remains scarce. By imposing Piola’s transformation [17, (2.1.69)], Qiu and Demkowicz [45] generalized the weakly symmetric Arnold-Falk-Winther element [7] to curved domains. Through extending polytopal template methods [48, 49], Sky, Neunteufel, Hale and Zilian [50] developed a novel fourth-order tensor-based polytopal transformation mapping Hu-Zhang basis functions from reference to physical elements. Such approach is also applicable to curved elements. For other problems with mixed methods, we refer readers to [8, 12, 14, 15, 27, 44, 55, 56] and the references therein.

This paper generalizes the Hu-Zhang element to curved triangulations while rigorously preserving strong symmetry and  $H(\text{div})$ -conformity. The loss of the polynomial nature of the curved Hu-Zhang element introduces significant challenges in analyzing the discrete inf-sup condition and establishing error estimates between the numerical solution and the exact solution. First, this non-polynomial structure makes it difficult to characterize the divergence space of  $H(\text{div})$  bubble function space, which is a critical step in proving the discrete inf-sup condition on simplicial meshes as established in [33, 37, 38]. Second, the deviation from polynomial exactness implies that the divergence space of the curved Hu-Zhang element is not contained in the discrete displacement space. This severely complicates the stress error estimate in the  $L^2$ -norm through standard arguments (such as those for simplicial meshes in [33, Remark 3.1]), particularly when geometric approximation errors coexist.

To overcome the first difficulty, we establish a novel discrete inf-sup condition on triangular meshes by substituting the  $H(\text{div})$ -norm of discrete stresses with a broken  $H^1$ -norm. This serves as a key step to recasting  $H(\text{div})$ -stability analysis on curved meshes as broken  $H^1$ -stability analysis on triangular meshes. The second difficulty is resolved by extending the mesh-dependent norm stability result for simplicial meshes, originally established in [23], to curved meshes. Moreover, a superclose estimate for the displacement follows directly from this extended stability framework. It is noteworthy that the failure of the inclusion (i.e.,  $\text{div } \Sigma_h^m \not\subset V_h^m$ ) introduces an error term in both stress  $L^2$ -error analysis and displacement superclose estimate, resulting in a half-order reduction from the optimal convergence rate (i.e., interpolation error order). Crucially, this degradation—unaffected by enhanced geometric approximation accuracy—is mitigated by locally increasing the polynomial degree of the curved Hu-Zhang element. This degree enhancement applies exclusively to boundary elements, only leading to a marginal increase in the total computation cost.

The rest of this paper is organized as follows. Section 1.1 introduces some key notations. Section 2 briefly reviews the Hu-Zhang element on triangular meshes, and Section 3 provides a quick review of curved triangulations. The extension of the Hu-Zhang element to curved meshes and proof of the discrete inf-sup condition are presented in Section 4, followed by error estimates in Sec-

tion 5. Finally, Section 6 provides numerical results validating the theoretical analysis.

### 1.1 Notations

For a bounded domain  $G \subset \mathbb{R}^2$  and a nonnegative integer  $m$ , denote the Sobolev space

$$H^m(G; \mathbb{X}) := \{\phi : G \rightarrow \mathbb{X} : D^\alpha \phi \in L^2(G; \mathbb{X}), |\alpha| \leq m\}, \quad (4)$$

where  $\mathbb{X}$  is a finite-dimensional vector space ( $\mathbb{X} = \mathbb{R}, \mathbb{R}^2$  or  $\mathbb{S}$ ). The associated norm and semi-norm are denoted by  $\|\cdot\|_{m,G}$  and  $|\cdot|_{m,G}$ , respectively. Further, for non-integer  $s$ , let  $H^s(G; \mathbb{X})$  be the intermediate spaces with norm  $\|\cdot\|_{s,G}$  by means of interpolation of Sobolev spaces of integer order. The  $L^2$  inner product on  $G$  is written as  $(\cdot, \cdot)_G$ . When  $G = \Omega$ , we simplify notation:  $\|\cdot\|_m := \|\cdot\|_{m,\Omega}$ ,  $|\cdot|_m := |\cdot|_{m,\Omega}$ ,  $\|\cdot\|_s := \|\cdot\|_{s,\Omega}$  and  $(\cdot, \cdot) := (\cdot, \cdot)_\Omega$ . Let  $H_0^m(G; \mathbb{R}^2)$  be the closure of  $C_0^\infty(G; \mathbb{R}^2)$  with respect to the norm  $\|\cdot\|_{m,G}$ . Define the Hilbert space for symmetric tensor fields with square-integrable divergence:

$$H(\operatorname{div}, G; \mathbb{S}) := \{\tau \in L^2(G; \mathbb{S}) : \operatorname{div} \tau \in L^2(G; \mathbb{R}^2)\}, \quad (5)$$

equipped with the following norm:

$$\|\tau\|_{H(\operatorname{div}, G)} := \left( \|\tau\|_{0,G}^2 + \|\operatorname{div} \tau\|_{0,G}^2 \right)^{\frac{1}{2}}, \quad \text{for all } \tau \in H(\operatorname{div}, G; \mathbb{S}). \quad (6)$$

Suppose  $\Omega$  is subdivided by a family of shape regular triangulations  $\mathcal{T}_h$  with  $h := \max_{K \in \mathcal{T}_h} h_K$  and  $h_K := \operatorname{diam}(K)$ . Let  $\mathcal{E}_h$  denote the union of all edges in  $\mathcal{T}_h$ , partitioned into boundary edges  $\mathcal{E}_{\partial,h}$  and interior edges  $\mathcal{E}_{0,h}$ . For any  $E \in \mathcal{E}_h$ , let  $h_E := \operatorname{diam}(E)$ , and fix a unit normal vector  $\nu_E$ . For  $\mathbb{X} \in \{\mathbb{R}, \mathbb{R}^2, \mathbb{S}\}$ , define  $P_m(G; \mathbb{X})$  as the space of polynomials of degree  $\leq m$  over  $G$  with values in  $\mathbb{X}$ . Let  $H^1(\mathcal{T}_h; \mathbb{X})$  be the broken Sobolev space over a triangulation  $\mathcal{T}_h$ :

$$H^1(\mathcal{T}_h; \mathbb{X}) := \left\{ v \in L^2(\Omega; \mathbb{X}) : \sum_{K \in \mathcal{T}_h} (\|v\|_{0,K}^2 + |v|_{1,K}^2) < \infty \right\}, \quad (7)$$

equipped with the element-wise  $H^1$ -norm:

$$\|v\|_{1,\mathcal{T}_h} := \left( \sum_{K \in \mathcal{T}_h} (\|v\|_{0,K}^2 + |v|_{1,K}^2) \right)^{\frac{1}{2}}, \quad \text{for all } v \in H^1(\mathcal{T}_h; \mathbb{X}). \quad (8)$$

For two adjacent triangles  $K^+, K^- \in \mathcal{T}_h$  sharing an interior edge  $E \in \mathcal{E}_{0,h}$ . Let  $\nu^+, \nu^-$  denote the unit outward normals to the common edge  $E$  of  $K^+$  and  $K^-$ , respectively. For a vector-valued function  $w$ , write  $w^+ := w|_{K^+}$  and  $w^- := w|_{K^-}$ . Then define the jump of  $w$  as

$$[[w]] := \begin{cases} w^+(\nu^+ \cdot \nu_E) + w^-(\nu^- \cdot \nu_E), & \text{if } E \in \mathcal{E}_{0,h}, \\ w, & \text{if } E \in \mathcal{E}_{\partial,h}. \end{cases} \quad (9)$$

Throughout this paper, the notation  $A \lesssim B$  denotes  $A \leq CB$ , where  $C > 0$  is a constant independent of the mesh size  $h$ . Similarly,  $A \approx B$  signifies  $A \lesssim B$  and  $B \lesssim A$ .

## 2 The Hu-Zhang element method

In the construction of the Hu-Zhang element space, the characterization of bubble functions constitutes the pivotal step. For each  $K \in \mathcal{T}_h$ , define the local  $H(\text{div})$ -conforming bubble function space:

$$\Sigma_{k,b}(K) := \{\tau \in P_k(K; \mathbb{S}) : \tau \cdot \nu|_{\partial K} = 0\}. \quad (10)$$

where  $\nu$  is the unit outer normal to  $\partial K$ . Denote the vertices of  $K$  by  $\mathbf{x}_{K,0}, \mathbf{x}_{K,1}$  and  $\mathbf{x}_{K,2}$  (abbreviated as  $\mathbf{x}_i$  when unambiguous). For each edge  $\mathbf{x}_i \mathbf{x}_j$  ( $i \neq j$ ), let  $t_{i,j}$  be the unit tangent vector along the edge. Define the symmetric tensors:

$$\mathbb{T}_{i,j} := t_{i,j} t_{i,j}^T, \quad 0 \leq i < j \leq 2.$$

As shown in [33, 37], the set  $\{\mathbb{T}_{i,j}\}_{0 \leq i < j \leq 2}$  forms a basis for  $\mathbb{S}$ , and

$$\Sigma_{k,b}(K) = \sum_{0 \leq i < j \leq 2} \lambda_i \lambda_j P_{k-2}(K, \mathbb{R}) \mathbb{T}_{i,j}, \quad (11)$$

where  $\lambda_i$  is the associated barycentric coordinate corresponding to  $\mathbf{x}_i$  for  $i = 0, 1, 2$ . The global Hu-Zhang element space  $\Sigma_h$  is defined as:

$$\begin{aligned} \Sigma_h := \{ \sigma \in H(\text{div}, \Omega; \mathbb{S}) : \sigma = \sigma_c + \sigma_b, \sigma_c \in H^1(\Omega; \mathbb{S}), \\ \sigma_c|_K \in P_k(K; \mathbb{S}), \sigma_b|_K \in \Sigma_{k,b}(K), \text{ for all } K \in \mathcal{T}_h \}, \end{aligned} \quad (12)$$

and the displacement space  $V_h$  as:

$$V_h := \{v \in L^2(\Omega; \mathbb{R}^2) : v|_K \in P_{k-1}(K; \mathbb{R}^2), \text{ for all } K \in \mathcal{T}_h\}. \quad (13)$$

The Hu-Zhang element method for (1) seeks  $(\sigma_h, u_h) \in \Sigma_h \times V_h$ , such that

$$\begin{cases} a(\sigma_h, \tau_h) + b(\tau_h, u_h) = 0, & \text{for all } \tau_h \in \Sigma_h, \\ b(\sigma_h, v_h) = -(f, v_h), & \text{for all } v_h \in V_h, \end{cases} \quad (14)$$

where  $a(\cdot, \cdot)$  and  $b(\cdot, \cdot)$  are defined in (2).

The error estimate of the Hu-Zhang element method is as follows [33, 37]:

$$\begin{aligned} \|\sigma - \sigma_h\|_{0,\Omega} + h\|\sigma - \sigma_h\|_{H(\text{div}, \Omega)} + h\|u - u_h\|_{0,\Omega} \\ \lesssim h^{k+1}(\|\sigma\|_{k+1,\Omega} + \|u\|_{k,\Omega}). \end{aligned} \quad (15)$$

Central to these results is the discrete inf-sup condition [33, Theorem 3.1], which guarantees: for any  $v_h \in V_h$ , there exists a  $\tau_h \in \Sigma_h$  satisfying

$$\text{div } \tau_h = v_h \text{ and } \|\tau_h\|_{H(\text{div}, \Omega)} \lesssim \|v_h\|_{0,\Omega}. \quad (16)$$

In this paper, a new inf-sup condition is established: there exists a  $\tau_h \in \Sigma_h$  satisfying  $\text{div } \tau_h = v_h$  and  $\|\tau_h\|_{1,\mathcal{T}_h} \lesssim \|v_h\|_{0,\Omega}$ , which is the critical component in analyzing the discrete inf-sup condition for the curved Hu-Zhang element method. The complete statement and rigorous proof are deferred to Section 4.3.2.

### 3 Triangulations with curved elements

When the domain  $\Omega$  has a curved boundary, the direct application of the Hu-Zhang element method on polygonal approximations of  $\Omega$  (via triangular meshes) to solve the linear elasticity problem (1) results in a suboptimal convergence rate for both stress and displacement. The loss in accuracy arises from geometric approximation errors inherent in piecewise linear representations of the boundary  $\partial\Omega$ . To recover the optimal convergence rate, we employ higher-order geometric approximations of  $\Omega$  through curved elements on the boundary.

We revisit the parametric framework for constructing  $m$ -th order curvilinear triangulations  $\mathcal{T}_h^m$  ( $m \geq 1$ ) to approximate the domain  $\Omega$  with a curved boundary, as established in [41] and described in [8]. The methodology initiates with a conforming, shape-regular, straight-edged triangulation  $\mathcal{T}_h^1$  with interior vertices belonging to  $\Omega$  and boundary vertices belonging to  $\partial\Omega$ . The approximate domain  $\Omega^1$  is the union of all elements in  $\mathcal{T}_h^1$ . Let  $\mathcal{T}_{\partial,h}^1$  denote the set of boundary triangles containing at least one edge on  $\partial\Omega^1$ . We impose the following assumption.

**Hypothesis 1** *Each triangle in  $\mathcal{T}_h^1$  has at most two vertices on the boundary  $\partial\Omega$ , and so it has at most one edge in  $\partial\Omega^1$ .*

Next, for each  $K^1 \in \mathcal{T}_h^1$ , we define a polynomial diffeomorphism  $F_K^m : K^1 \rightarrow \mathbb{R}^2$  of degree  $m$  that maps  $K^1$  onto a curvilinear triangle  $K^m$ . This mapping is constructed as follows. All interior edges remain fixed, preserving conformity. The boundary edge is determined by interpolating a parametric chart of  $\partial\Omega$ . The interior element points are defined via the barycentric coordinate interpolation. See equation (14) of [41] for an explicit formula for  $F_K^m \circ \widehat{F}_K^1$ , where  $\widehat{F}_K^1$  is the affine mapping from the standard reference triangle to  $K^1$ . The mapping  $F_K^m$  satisfies the optimal  $L^\infty$ -bound on its derivatives, as established in [41, Theorems 1-2]. Furthermore, the resulting order- $m$  curvilinear triangulation

$$\mathcal{T}_h^m := \{K^m = F_K^m(K^1) : K^1 \in \mathcal{T}_h^1\} \quad (17)$$

is a conforming, shape-regular triangulation that approximates  $\Omega$  by  $\Omega^m := \bigcup_{K^m \in \mathcal{T}_h^m} K^m$ . Extending the notation for  $m = 1$  in Section 2, we also denote by  $\mathcal{E}_h^m$  the set of edges of triangulation  $\mathcal{T}_h^m$ .  $\mathcal{E}_h^m$  is partitioned into interior edges  $\mathcal{E}_{0,h}^m$  (all straight) and boundary edges  $\mathcal{E}_{\partial,h}^m$  (possibly curved). Thus, the reconstructed boundary  $\partial\Omega^m := \bigcup_{E^m \in \mathcal{E}_{\partial,h}^m} E^m$  is an  $m$ -th order approximation of  $\partial\Omega$ . The parametric mapping satisfies three conditions: 1.  $F_K^1 \equiv \text{id}_{K^1}$ ; 2. if  $K^1$  has no edge on  $\partial\Omega^1$ , then  $F_K^m \equiv \text{id}_{K^1}$ ; and 3.  $F_K^m|_E = \text{id}_{K^1}|_E$  for all interior edges  $E \in \mathcal{E}_{0,h}^m$ . Denote by  $\mathcal{T}_{\partial,h}^m$  the set of all boundary triangles and by  $\mathcal{T}_{i,h}^m$  the set of all inner triangles. Let  $\Omega_S^m := \bigcup_{K^m \in \mathcal{T}_{\partial,h}^m} K^m$  denote the union of all boundary triangles. It satisfies the inclusion

$$\Omega_S^m \subset \Omega_h^m := \{x \in \Omega^m : \exists y \in \partial\Omega^m, \text{dist}(x, y) \leq h\}, \quad (18)$$

where  $\text{dist}(x, y)$  is the distance between  $x$  and  $y$ . Thus, by [18, Lemma 2.2], the following inequality holds for  $0 \leq s \leq \frac{1}{2}$ .

$$\|v\|_{0, \Omega^m} \lesssim h^s \|v\|_{s, \Omega^m}, \quad \text{for all } v \in H^s(\Omega^m). \quad (19)$$

The local polynomial diffeomorphisms  $\{F_K^m\}_{K \in \mathcal{T}_h^1}$  naturally induce a global piecewise polynomial mapping:

$$F^m : \Omega^1 \rightarrow \Omega^m, \quad F^m|_K := F_K^m, \quad \text{for all } K \in \mathcal{T}_h^1. \quad (20)$$

Furthermore, for any two approximation orders  $1 \leq l \leq m < \infty$ , we define the composite mapping between corresponding approximate domains:  $\Phi^{lm} : \Omega^l \rightarrow \Omega^m$ , constructed piecewise

$$\Phi^{lm}|_{K^l} := \Phi_K^{lm} := F_K^m \circ (F_K^l)^{-1}, \quad \text{for all } K^l \in \mathcal{T}_h^l. \quad (21)$$

To compare the exact solution defined on the physical domain  $\Omega$  and its numerical approximation defined on the approximate domain  $\Omega^m$ , we establish an element-wise mapping from  $\Omega^m$  to  $\Omega$ . Specifically, for each element  $K^m \in \mathcal{T}_h^m$ , we construct a diffeomorphic mapping  $\Psi_K^m : K^m \rightarrow \mathbb{R}^2$  that transforms the parametric triangle  $K^m$  into a curvilinear triangle  $K$  precisely conforming to  $\partial\Omega$ . Following the framework in [41], we implement this mapping as follows: For interior elements without boundary edges, the mapping reduces to the identity transformation. For boundary elements containing an edge  $E^m \subset \partial\Omega^m$ , the mapping is explicitly defined through the parametric equations in [41, eq. (32)], ensuring exact geometric matching. This element-wise construction generates a curvilinear triangulation  $\mathcal{T}_h := \{\Psi_K^m(K^m)\}_{K^m \in \mathcal{T}_h^m}$  that exactly preserves the physical domain geometry. The local mappings  $\Psi_K^m$  can be aggregated through a partition-of-unity approach to form a global mapping  $\Psi^m : \Omega^m \rightarrow \Omega$ .

The exact domain  $\Omega$  and its triangulation  $\mathcal{T}_h$  can be conceptually framed as the limiting case of the approximate domain sequence  $\{\Omega^m\}_{m \geq 1}$  and their triangulations  $\{\mathcal{T}_h^m\}_{m \geq 1}$  as  $m \rightarrow \infty$ . The interpretive framework motivates the adoption of alternative notations:  $\Omega^\infty \equiv \Omega$ ,  $\mathcal{T}_h^\infty \equiv \mathcal{T}_h$ ,  $\Phi^{l\infty} \equiv \Psi^l$ ,  $F_K^\infty \equiv \Psi^1$ , etc., which will sometimes be convenient.

The following theorem, adapted from [8, Theorem 3.2], serves as the fundamental framework for both stability analysis and error estimates in the curved Hu-Zhang element method.

**Theorem 1** *Assume Hypothesis 1. Then for all  $1 \leq l \leq m \leq r$  and  $m = \infty$ , mappings  $\Phi^{lm}$  described above satisfy*

$$\begin{aligned} \|\nabla^s(\Phi_K^{lm} - \text{id}_{K^l})\|_{L^\infty(K^l)} &\lesssim h^{l+1-s}, \quad \text{for all } 0 \leq s \leq l+1, \\ \|\nabla^s((\Phi_K^{lm})^{-1} - \text{id}_{K^m})\|_{L^\infty(K^m)} &\lesssim h^{l+1-s}, \quad \text{for all } 0 \leq s \leq l+1, \end{aligned} \quad (22)$$

where all constants depend on the piecewise  $C^{r+1}$  norm of  $\partial\Omega$ .

We conclude this section with some basic results, which follow directly from the chain rule and Theorem 1.

**Proposition 1** For all  $1 \leq l \leq m \leq r$  and  $m = \infty$ , let  $v \in H^s(K^m; \mathbb{X})$  with  $\mathbb{X} \in \{\mathbb{R}, \mathbb{R}^2, \mathbb{S}\}$ ,  $\tau \in H^1(K^m; \mathbb{S})$ ,  $\hat{v} = v \circ \Phi_K^{lm} \in H^s(K^l; \mathbb{X})$  and  $\hat{\tau} = \tau \circ \Phi_K^{lm} \in H^1(K^l; \mathbb{S})$ . Assume Hypothesis 1, then

$$\|v\|_{s,K^m} \approx \|\hat{v}\|_{s,K^l}, \quad \text{for all } 0 \leq s \leq l+1. \quad (23)$$

$$\|(\operatorname{div} \tau) \circ \Phi_K^{lm} - \operatorname{div} \hat{\tau}\|_{0,K^l} \lesssim h^l |\hat{\tau}|_{1,K^l}, \quad (24)$$

$$\|\operatorname{div} \tau - (\operatorname{div} \hat{\tau}) \circ (\Phi_K^{lm})^{-1}\|_{0,K^m} \lesssim h^l |\tau|_{1,K^m}, \quad (25)$$

where all constants depend on the piecewise  $C^{r+1}$  norm of  $\partial\Omega$ .

#### 4 The curved Hu-Zhang element method

This section generalizes the Hu-Zhang element to curved meshes through the parametric diffeomorphic mapping  $F^m$ , and establishes the well-posedness of the discrete formulation. Hereafter, unless otherwise specified, we perpetually enforce Hypothesis 1.

##### 4.1 The curved Hu-Zhang element space

Let  $m \geq 1$  denote the geometric approximation order. For  $k \geq 3$ , we introduce the  $k$ -th order finite element space over the curvilinear triangulation  $\mathcal{T}_h^m$ , which begins with the finite element spaces  $\Sigma_h^1$  and  $V_h^1$  on  $\mathcal{T}_h^1$ , defined in (12) and (13), respectively.

The stress space  $\Sigma_h^m$  and displacement space  $V_h^m$  over domain  $\Omega^m$  are defined via the mapping  $F^m$  as

$$\begin{aligned} \Sigma_h^m &:= \{\sigma \in L^2(\Omega^m; \mathbb{S}) : \sigma = \sigma_c + \sigma_b, \sigma_c \in H^1(\Omega^m; \mathbb{S}), \\ &\quad \sigma_c|_{K^m} \circ F_K^m \in P_k(K^1; \mathbb{S}), \sigma_b|_{K^m} \in \Sigma_{k,b}(K^m), \text{ for all } K^m \in \mathcal{T}_h^m\}, \end{aligned} \quad (26)$$

$$V_h^m := \{v \in L^2(\Omega^m; \mathbb{R}^2) : v \circ F^m \in V_h^1\}. \quad (27)$$

Here  $\Sigma_{k,b}(K^m)$  is defined as

$$\Sigma_{k,b}(K^m) := \{\tau \in L^2(K^m; \mathbb{S}) : \tau \circ F_K^m \in \Sigma_{k,b}(K^1)\}, \quad (28)$$

where  $\Sigma_{k,b}(K^1)$  is the  $H(\operatorname{div}, K^1; \mathbb{S})$  bubble function space in (11). When  $K^m$  is an inner element ( $F_K^m \equiv \operatorname{id}_{K^1}$ ),  $\Sigma_{k,b}(K^m) = \Sigma_{k,b}(K^1)$  is the full  $H(\operatorname{div}, K^m; \mathbb{S})$  bubble function space. For the boundary element  $K^m$ , consider any interior edge  $E \subset \partial K^m$  where the parametrization mapping satisfies  $F_K^m|_E = \operatorname{id}_{K^1}|_E$ . This induces

$$\tau \cdot \nu|_E = 0, \quad \text{for all } \tau \in \Sigma_{k,b}(K^m). \quad (29)$$

Consequently, the normal component of  $\tau$  vanishes on all interior edges. This, combined with (26), indicates that  $\Sigma_h^m$  is a conforming subspace of  $H(\operatorname{div}, \Omega^m; \mathbb{S})$ .

*Remark 1* In fact, we have

$$\Sigma_h^m = \{\sigma \in H(\operatorname{div}, \Omega^m; \mathbb{S}) : \sigma \circ F^m \in \Sigma_h^1\}. \quad (30)$$



#### 4.2 Mixed formulations of the curved Hu-Zhang element

To construct the mixed variational formulation over the curved triangulation  $\mathcal{T}_h^m$ , we extend the bilinear forms in (2) to parameter-dependent counterparts  $a^m(\cdot, \cdot)$  and  $b^m(\cdot, \cdot)$ ,

$$a^m(\sigma, \tau) := (\mathcal{A}\sigma, \tau)_{\Omega^m}, \quad b^m(\tau, v) := (\operatorname{div} \tau, v)_{\Omega^m}. \quad (31)$$

The mixed finite element approximation to (1) is: find  $(\sigma_h, u_h) \in \Sigma_h^m \times V_h^m$  such that

$$\begin{cases} a^m(\sigma_h, \tau_h) + b^m(\tau_h, u_h) = 0, & \text{for all } \tau_h \in \Sigma_h^m, \\ b^m(\sigma_h, v_h) = -(\tilde{f}, v_h)_{\Omega^m}, & \text{for all } v_h \in V_h^m, \end{cases} \quad (32)$$

with  $\tilde{f} = f \circ \Psi^m \det(\nabla \Psi^m)$ . The well-posedness of the discrete problem (32) will be rigorously established in the following section. Spaces and corresponding norms over the approximate domain  $\Omega^m$ , including  $H(\operatorname{div}, \Omega^m; \mathbb{S})$  and  $H^1(\mathcal{T}_h^m; \mathbb{X})$ , are defined analogously to those in (5)–(6) and (7)–(8), respectively. This subsection concludes with the following geometric approximation lemma, which is critical for stability and error analysis.

**Lemma 1** *Let  $1 \leq l \leq r$  such that  $m > l$ ,  $\Phi \equiv \Phi^{lm} : \Omega^l \rightarrow \Omega^m$  from (21) for  $1 < m \leq r$  and  $m = \infty$ . For any  $\sigma, \tau \in H(\operatorname{div}, \Omega^m; \mathbb{S})$  and  $v \in L^2(\Omega^m; \mathbb{R}^2)$ , define their pullbacks  $\hat{\sigma} = \sigma \circ \Phi$ ,  $\hat{\tau} = \tau \circ \Phi$  and  $\hat{v} = v \circ \Phi$ . The following estimate holds:*

$$|a^m(\sigma, \tau) - a^l(\hat{\sigma}, \hat{\tau})| \lesssim h^l \|\hat{\sigma}\|_{0, \Omega_S^l} \|\hat{\tau}\|_{0, \Omega_S^l}. \quad (33)$$

Furthermore, if  $\sigma \in H(\operatorname{div}, \Omega^m; \mathbb{S}) \cap H^1(\mathcal{T}_h^m; \mathbb{S})$ ,

$$|b^m(\sigma, v) - b^l(\hat{\sigma}, \hat{v})| \lesssim h^l \|\hat{\nabla}_h \hat{\sigma}\|_{0, \Omega_S^l} \|\hat{v}\|_{0, \Omega_S^l}, \quad (34)$$

and if  $v \in H^1(\mathcal{T}_h^m; \mathbb{R}^2)$ ,

$$\begin{aligned} |b^m(\sigma, v) - b^l(\hat{\sigma}, \hat{v})| &\lesssim h^l \|\hat{\sigma}\|_{0, \Omega_S^l} \|\hat{\nabla}_h \hat{v}\|_{0, \Omega_S^l} \\ &+ h^l \left( \sum_{E^l \in \mathcal{E}_{\partial, h}^l} h_{E^l} \|\hat{\sigma} \hat{n}\|_{L^2(E^l)}^2 \right)^{\frac{1}{2}} \left( \sum_{E^l \in \mathcal{E}_{\partial, h}^l} h_{E^l}^{-1} \|\hat{v}\|_{L^2(E^l)}^2 \right)^{\frac{1}{2}}, \end{aligned} \quad (35)$$

where  $\hat{\nabla}_h$  is the broken gradient operator over  $\mathcal{T}_h^l$ .

*Proof* Let  $J = \hat{\nabla}_h \Phi$  be the element-wise Jacobian of the parametric mapping. By transforming the integrals of the bilinear forms  $a^m(\sigma, \tau)$  and  $b^m(\sigma, v)$  from  $\Omega^m$  to  $\Omega^l$ , we derive consistency errors on each element:

$$(\mathcal{A}\sigma, \tau)_{K^m} - (\mathcal{A}\hat{\sigma}, \hat{\tau})_{K^l} = (\mathcal{A}\hat{\sigma}, \hat{\tau}(\det(J) - 1))_{K^l}, \quad (36)$$

and

$$\begin{aligned} (\operatorname{div} \sigma, v)_{K^m} - (\operatorname{div} \hat{\sigma}, \hat{v})_{K^l} \\ = (\widehat{\operatorname{div} \sigma} - \hat{\operatorname{div}} \hat{\sigma}, \hat{v} \det(J))_{K^l} + (\hat{\operatorname{div}} \hat{\sigma}, \hat{v}(\det(J) - 1))_{K^l}. \end{aligned} \quad (37)$$

By applying integration by parts and using  $\Phi|_E = \text{id}_{K^l}|_E$  on interior edges, we obtain:

$$\begin{aligned} & (\text{div } \sigma, v)_{K^m} - (\hat{\text{div}} \hat{\sigma}, \hat{v})_{K^l} \\ &= -(\hat{\sigma}, [\widehat{\varepsilon(v)} - \hat{\varepsilon}(\hat{v})] \det(J))_{K^l} - (\hat{\sigma}, \hat{\varepsilon}(\hat{v})(\det(J) - 1))_{K^l} \\ &+ (\hat{\sigma}(J^{-T} - \text{I})\hat{n}, \hat{v} \det(J))_{\partial K^l \cap \partial \Omega^l} + (\hat{\sigma}\hat{n}, \hat{v}(\det(J) - 1))_{\partial K^l \cap \partial \Omega^l}. \end{aligned} \quad (38)$$

Since  $J = \text{I}$  holds for all interior triangles, the estimates in (33), (34) and (35) follow from combining (36), (37) and (38) with the parametric bound in (22) and applications of the weighted Cauchy-Schwarz inequality.

### 4.3 Well-posedness analysis

Following the abstract stability theory for mixed finite element methods [17], we need to verify two fundamental conditions with mesh-independent constants:

1. K-ellipticity.

$$a^m(\tau, \tau) \gtrsim \|\tau\|_{H(\text{div}, \Omega^m)}^2, \quad \text{for all } \tau \in \mathcal{Z}_h^m, \quad (39)$$

where the discrete kernel space  $\mathcal{Z}_h^m$  is defined as:

$$\mathcal{Z}_h^m := \{\tau \in \Sigma_h^m : b^m(\tau, v) = 0, \text{ for all } v \in V_h^m\}. \quad (40)$$

2. Discrete inf-sup condition.

$$\sup_{0 \neq \tau \in \Sigma_h^m} \frac{b^m(\tau, v)}{\|\tau\|_{H(\text{div}, \Omega^m)}} \gtrsim \|v\|_{0, \Omega^m}, \quad \text{for all } v \in V_h^m. \quad (41)$$

#### 4.3.1 K-ellipticity

Let  $Q_h : L^2(\Omega^m; \mathbb{R}^2) \rightarrow V_h^m$  denote the orthogonal projection operator with respect to the  $L^2$ -inner product. The following lemma establishes the K-ellipticity of  $a^m(\cdot, \cdot)$  over the discrete kernel space  $\mathcal{Z}_h^m$ .

**Lemma 2** *For any  $\tau \in \Sigma_h^m$ , it holds that*

$$\|(I - Q_h) \text{div } \tau\|_{0, K^m} \lesssim \min \{h|\tau|_{1, K^m}, \|\tau\|_{0, K^m}\}, \quad \text{for all } K^m \in \mathcal{T}_h^m. \quad (42)$$

*Proof* For any interior element  $K^m \in \mathcal{T}_h^m$ , the divergence constraint implies  $\text{div } \tau|_{K^m} \in P_{k-1}(K^m; \mathbb{R}^2)$ . Since  $Q_h$  preserves polynomials of degree  $k-1$ , that is,  $Q_h|_{K^m} = I|_{K^m}$ , the bound (42) holds trivially. Let  $K^m \in \mathcal{T}_h^m$  be a boundary element. Define the pulled-back tensor field  $\hat{\tau} := \tau|_{K^m} \circ F_K^m$  and let  $v := \hat{\text{div}} \hat{\tau} \circ (F_K^m)^{-1}$ . Then

$$\begin{aligned} \|(I - Q_h) \text{div } \tau\|_{0, K^m} &= \|(I - Q_h)(\text{div } \tau - v)\|_{0, K^m} \\ &\leq \|\text{div } \tau - \hat{\text{div}} \hat{\tau} \circ (F_K^m)^{-1}\|_{0, K^m}. \end{aligned} \quad (43)$$

The combination of the parametric divergence estimate (25) at  $l = 1$ , and the polynomial inverse inequality [20, Lemma 4.5.3], establishes (42) for boundary elements, which completes the proof.

The definition of the kernel space (40) implies that  $(I - Q_h) \operatorname{div} \tau = \operatorname{div} \tau$  holds for all  $\tau \in \mathcal{Z}_h^m$ . This, combined with Lemma 2, yields  $\|\operatorname{div} \tau\|_{0,\Omega^m} \lesssim \|\tau\|_{0,\Omega^m}$ . Consequently, the K-ellipticity condition (39) is verified.

#### 4.3.2 Discrete inf-sup condition

For  $m \geq 2$ , the non-polynomial structure of  $\Sigma_h^m$  and  $V_h^m$  on boundary element  $K^m$  introduces intrinsic analytical difficulties in analyzing the discrete inf-sup condition. This challenge originates from the inherent difficulty in establishing a precise characterization of the divergence space associated with the bubble function space  $\Sigma_{k,b}(K^m)$ , analogous to the structural results achieved for polynomial-based settings in [33, Theorem 2.2].

The key to overcoming the aforementioned challenge lies in the following theorem. By lifting the  $H(\operatorname{div})$ -norm in (16) to the broken  $H^1$ -norm, this theorem enables us to establish the discrete inf-sup condition on  $\mathcal{T}_h^m$  through the error estimate between  $b^m(\cdot, \cdot)$  and  $b^1(\cdot, \cdot)$ . The proof follows a methodology similar to that in [23, 33], and can be divided into two main steps: see Lemma 3 and Lemma 4 for details. It is worth noting that a mesh-dependent norm inf-sup condition introduced in [23]—here adapted to its curved-boundary element version—will be employed in deriving the  $L^2$ -error estimate for the stress in Section 5.3.

**Theorem 2** *For any  $v_h \in V_h^1$ , there exists a  $\tau_h \in \Sigma_h^1$ , such that*

$$\operatorname{div} \tau_h = v_h \quad \text{and} \quad \|\tau_h\|_{1,\mathcal{T}_h^1} \lesssim \|v_h\|_{0,\Omega^1}. \quad (44)$$

Before proving Theorem 2, we introduce the following rigid motion space on each element  $K^1 \in \mathcal{T}_h^1$ .

$$R(K^1) := \{v \in H^1(K^1; \mathbb{R}^2) : (\nabla v + \nabla v^T)/2 = 0\}. \quad (45)$$

It follows from the definition that  $R(K^1)$  is a subspace of  $P_1(K^1; \mathbb{R}^2)$ . This allows for defining the orthogonal complement space of  $R(K^1)$  with respect to  $P_{k-1}(K^1; \mathbb{R}^2)$  by

$$R^\perp(K^1) := \{v \in P_{k-1}(K^1; \mathbb{R}^2) : (v, w)_{K^1} = 0, \text{ for all } w \in R(K^1)\}. \quad (46)$$

According to [33, Theorem 2.2], the divergence space of  $\Sigma_{k,b}(K^1)$  satisfies

$$\operatorname{div} \Sigma_{k,b}(K^1) = R^\perp(K^1), \quad \text{for all } K^1 \in \mathcal{T}_h^1. \quad (47)$$

This intrinsic property facilitates the subsequent lemma concerning discrete stability.

**Lemma 3** *For any  $v \in R^\perp(K^1)$ , there exists a  $\tau \in \Sigma_{k,b}(K^1)$ , such that*

$$\operatorname{div} \tau = v \quad \text{and} \quad \|\tau\|_{1,K^1} \lesssim \|v\|_{0,K^1}. \quad (48)$$

*Proof* Choosing  $\tau \in \Sigma_{k,b}(K^1)$ , such that

$$\operatorname{div} \tau = v \text{ and } \|\tau\|_{0,K} = \min\{\|\tau\|_{0,K} : \operatorname{div} \tau = v, \tau \in \Sigma_{k,b}(K^1)\}. \quad (49)$$

Let  $F$  be the affine mapping from reference element  $\hat{K}$  to  $K^1$ , denoted by  $F(\hat{x}) = B\hat{x} + b$ , where  $B$  is an invertible matrix and  $b$  is a translation vector determined by  $K^1$ . Let  $\hat{\tau} \in \Sigma_{k,b}(\hat{K})$  be the matrix Piola transform of  $\tau$  by  $\tau(x) := B\hat{\tau}(\hat{x})B^T$ . A direct computation shows that  $\operatorname{div} \tau(x) = B\operatorname{div} \hat{\tau}(\hat{x})$ . The invertibility of  $B$  and the definition of  $\tau$  imply that  $\|\operatorname{div} \hat{\tau}\|_{0,\hat{K}}$  is a well-defined norm. Applying the norm equivalence theorem (valid for finite-dimensional spaces) and a scaling argument, we derive  $\|\tau\|_{1,K^1} \leq C\|\operatorname{div} \tau\|_{0,K^1} = C\|v\|_{0,K^1}$ , where  $C > 0$  is a constant depending on the shape regularity of  $K^1$ , which completes the proof.

By [33, Lemma 3.1], for any  $v_h \in V_h^1$ , there exists a  $\tau_h \in \Sigma_h^1 \cap H^1(\Omega^1; \mathbb{S})$  satisfying the orthogonality condition:

$$(\operatorname{div} \tau_h - v_h, p)_{K^1} = 0, \quad \text{for all } p \in R(K^1), \quad K^1 \in \mathcal{T}_h^1. \quad (50)$$

with the stability estimate  $\|\tau_h\|_{H(\operatorname{div}, \Omega^1)} \lesssim \|v_h\|_{0,\Omega^1}$ . One observation is that the stability persists when replacing the  $H(\operatorname{div})$ -norm with the stronger  $H^1$ -norm, i.e.,  $\|\tau_h\|_{1,\Omega^1} \leq C\|v_h\|_{0,\Omega^1}$ . This stems from the proof structure in [33, Lemma 3.1] where both components of  $\tau_h$  (interpolation part and correction part) can be controlled by  $\|v_h\|_{0,\Omega^1}$ . Integrating these analytical components, we can establish the following lemma to control the rigid motion part of  $v_h$ .

**Lemma 4** *For any  $v_h \in V_h^1$ , there exists a  $\tau_h \in \Sigma_h^1 \cap H^1(\Omega^1; \mathbb{S})$  such that, for all  $p \in R(K^1)$ , and  $K^1 \in \mathcal{T}_h^1$ ,*

$$(\operatorname{div} \tau_h - v_h, p)_{K^1} = 0 \quad \text{and} \quad \|\tau_h\|_{1,\Omega^1} \lesssim \|v_h\|_{0,\Omega^1}. \quad (51)$$

Now we prove Theorem 2 in two steps. First, select  $\tau_1 \in \Sigma_h^1$  via Lemma 4, such that

$$(v_h - \operatorname{div} \tau_1)|_{K^1} \in R^\perp(K^1), \quad \text{for all } K^1 \in \mathcal{T}_h^1. \quad (52)$$

Second, by Lemma 3, there exists a  $\tau_2 \in \Sigma_h^1$  with  $\tau_2|_{K^1} \in \Sigma_{k,b}(K^1)$  satisfying

$$\operatorname{div} \tau_2 = v_h - \operatorname{div} \tau_1 \quad \text{and} \quad \|\tau_2\|_{1,\mathcal{T}_h^1} \lesssim \|v_h - \operatorname{div} \tau_1\|_{0,\Omega^1}. \quad (53)$$

The composite stress  $\tau_h = \tau_1 + \tau_2$  then verifies

$$\operatorname{div} \tau_h = v_h \quad \text{and} \quad \|\tau_h\|_{1,\mathcal{T}_h^1} \lesssim \|v\|_{0,\Omega^1}, \quad (54)$$

which completes the proof of Theorem 2.

We are in the position to show the discrete inf-sup condition (41) for  $m > 1$ .

**Theorem 3** *For any  $v \in V_h^m$ , there exists a  $\tau \in \Sigma_h^m$ , such that for all sufficiently small mesh size  $h$ ,*

$$b^m(\tau, v) \gtrsim \|v\|_{0,\Omega^m}^2 \quad \text{and} \quad \|\tau\|_{1,\mathcal{T}_h^m} \lesssim \|v\|_{0,\Omega^m}, \quad (55)$$

where the constant is independent of both  $h$  and  $m$ . Consequently, the inf-sup condition (41) holds.

*Proof* For  $v \in V_h^m$  and  $\hat{v} = v \circ F_h^m \in V_h^1$ . By Theorem 2, there is a  $\hat{\tau} \in \Sigma_h^1$  satisfying

$$\operatorname{div} \hat{\tau} = \hat{v} \quad \text{and} \quad \|\hat{\tau}\|_{1, \mathcal{T}_h^1} \leq C \|\hat{v}\|_{0, \Omega^1}. \quad (56)$$

Let  $\tau = \hat{\tau} \circ (F_h^m)^{-1}$ . It follows from (34) and (23) with  $l = 1$  that

$$b^m(\tau, v) \geq \|\hat{v}\|_{0, \Omega^1}^2 - Ch \|\hat{\tau}\|_{1, \mathcal{T}_h^1} \|\hat{v}\|_{0, \Omega^1} \geq (1 - Ch) \|v\|_{0, \Omega^m}^2. \quad (57)$$

For sufficiently small  $h$ , we obtain the first inequality in (55). The second inequality in (55) follows from  $\|\tau\|_{1, \mathcal{T}_h^m} \lesssim \|\hat{\tau}\|_{1, \mathcal{T}_h^1} \lesssim \|v\|_{0, \Omega^m}$ , which completes the proof.

*Remark 2* The discrete mixed formulation (32) can be reformulated in terms of the monolithic bilinear form:

$$\mathbb{A}^m(\sigma_h, u_h; \tau_h, v_h) = -(\tilde{f}, v_h)_{\Omega^m}, \quad (58)$$

where  $\mathbb{A}^m(\sigma_h, u_h; \tau_h, v_h) := a^m(\sigma_h, \tau_h) + b^m(\tau_h, u_h) + b^m(\sigma_h, v_h)$ . The K-ellipticity (39) and the discrete inf-sup condition (41) yield the stability result,

$$\|\sigma_h\|_{H(\operatorname{div}, \Omega^m)} + \|u_h\|_{0, \Omega^m} \lesssim \sup_{(\tau_h, v_h) \in \Sigma_h^m \times V_h^m} \frac{\mathbb{A}^m(\sigma_h, u_h; \tau_h, v_h)}{\|\tau_h\|_{H(\operatorname{div}, \Omega^m)} + \|v_h\|_{0, \Omega^m}}. \quad (59)$$

This inequality will be used in the error estimates derived in the next section.

## 5 Error analysis

The error analysis of the curved Hu-Zhang element method faces an intrinsic difficulty: the divergence space of the curved Hu-Zhang element is not contained in the discrete displacement space (i.e.,  $\operatorname{div} \Sigma_h^m \not\subset V_h^m$ ), which precludes a direct error estimate of stress in the  $L^2$ -norm through standard arguments like those for simplicial meshes in [33, Remark 3.1]. To circumvent this, we introduce mesh-dependent norms in the  $L^2$ -error analysis. It is noteworthy that, such non-inclusion property introduces a consistency error that reduces the stress convergence rate by half an order compared to the optimal rate. Crucially, the suboptimality, rooted in incompatibility of the approximation space, can be eliminated by increasing the polynomial degree on boundary elements in the discretization scheme. This adjustment restores optimal convergence rates, as numerically demonstrated in the next section.

Compared with the case that  $\Omega$  is a polygonal region, the geometric approximation curved boundary  $\partial\Omega$  introduces a nonconforming error, which in turn deteriorates the final convergence order of the finite element solution. To analyze the geometric error, we will use the following inequality, which corresponds to  $s = \frac{1}{2}$  in (19).

$$\|v\|_{0, \Omega_S^m} \lesssim h^{\frac{1}{2}} \|v\|_{\frac{1}{2}, \Omega^m}, \quad \text{for all } v \in H^{\frac{1}{2}}(\Omega^m). \quad (60)$$

### 5.1 The geometric error

We begin with estimating the error caused by geometric approximation, specifically the error of the substitution of the exact solution into the variational formulation defined on the approximated domain  $\Omega^m$ .

**Lemma 5** *Recall the mapping  $\Psi^m : \Omega^m \rightarrow \Omega$  with  $\Psi_K^m := \Psi^m|_K$  from Section 3. Let  $(\sigma, u)$  be the solutions of (1) on the physical domain  $\Omega$ . Let  $\hat{\sigma} := \sigma \circ \Psi^m$  and  $\hat{u} := u \circ \Psi^m$  denote the pull-back of  $\sigma$  and  $u$ , respectively. Suppose  $u \in H^{s+1}(\Omega; \mathbb{R}^2)$  with  $s \geq \frac{3}{2}$ , such that  $\sigma \in H^s(\Omega^m; \mathbb{S})$ . Then we obtain the equation for the geometric error:*

$$\mathbb{A}^m(\hat{\sigma}, \hat{u}; \hat{\tau}, \hat{v}) = -(\tilde{f}, \hat{v})_{\Omega^m} + E(\hat{\tau}, \hat{v}), \quad (61)$$

for all  $\hat{\tau} = \tau \circ \Psi^m$  and  $\hat{v} = v \circ \Psi^m$  with  $(\tau, v) \in \Sigma \times V$ , where

$$|E(\hat{\tau}, \hat{v})| \lesssim h^{m+\frac{1}{2}} (\|\hat{\tau}\|_{0, \Omega_S^m} + \|\hat{v}\|_{0, \Omega_S^m}) \|u\|_{H^{\frac{5}{2}}(\Omega)}. \quad (62)$$

*Proof* By the variational formulation (1) and the definition of  $\mathbb{A}^m$ ,

$$\begin{aligned} E(\hat{\tau}, \hat{v}) &= [a^m(\hat{\sigma}, \hat{\tau}) - a(\sigma, \tau)] \\ &\quad + [b^m(\hat{\tau}, \hat{u}) - b(\tau, u)] + [b^m(\hat{\sigma}, \hat{v}) - b(\sigma, v)]. \end{aligned} \quad (63)$$

By using the estimates from (33), (34) and (35) through the parameter substitution  $(m, l) \rightarrow (\infty, m)$ , and applying the boundary condition  $\hat{u}|_{\partial\Omega^m} = 0$ , we derive the error bound:

$$|E(\hat{\tau}, \hat{v})| \lesssim h^m (\|\hat{\tau}\|_{0, \Omega_S^m} + \|\hat{v}\|_{0, \Omega_S^m}) (\|\hat{\sigma}\|_{H^1(\Omega_S^m)} + \|\hat{u}\|_{H^1(\Omega_S^m)}). \quad (64)$$

This, combined with (60) and (23), completes the proof.

For technical reasons, we impose a relatively strong regularity assumption  $s \geq \frac{3}{2}$  on the solution at this point. In fact, similar results can still be obtained when the solution has lower regularity, although with a possible loss of half an order. Therefore, in the following analysis, we always assume that the solutions satisfy the regularity condition with  $s \geq \frac{3}{2}$ .

### 5.2 The finite element error

Lemma 5 establishes a direct method for estimating the  $H(\text{div})$ -norm error of the stress  $\sigma$  and the  $L^2$ -norm error of the displacement  $u$ .

**Theorem 4** *Let  $(\sigma, u)$  be the solutions of (1), and  $(\hat{\sigma}_h, \hat{u}_h) \in \Sigma_h^m \times V_h^m$  are the discrete solutions of (58). Then, the following error estimate holds:*

$$\|\hat{\sigma} - \hat{\sigma}_h\|_{H(\text{div}, \Omega^m)} + \|\hat{u} - \hat{u}_h\|_{0, \Omega^m} \lesssim h^q \|u\|_{H^{q+2}(\Omega)}, \quad (65)$$

where the convergence order  $q = \min\{k, m + \frac{1}{2}, s - 1\}$ . The constant depends on  $\Omega$ , the compliance tensor  $\mathcal{A}$  and the shape regularity of  $\mathcal{T}_h^m$ .

*Proof* Starting from the variational formulation in (58) and (61), for any  $(\hat{\tau}_h, \hat{v}_h) \in \Sigma_h^m \times V_h^m$ , we derive the following equation:

$$\mathbb{A}^m(\hat{\sigma}_h, \hat{u}_h; \hat{\tau}_h, \hat{v}_h) = \mathbb{A}^m(\hat{\sigma}, \hat{u}; \hat{\tau}_h, \hat{v}_h) - E(\hat{\tau}_h, \hat{v}_h). \quad (66)$$

Let  $(\hat{\sigma}_I, \hat{u}_I)$  be the parametric interpolation of  $(\hat{\sigma}, \hat{u})$  to  $\Sigma_h^m \times V_h^m$ , defined by  $\hat{\sigma}_I \circ F^m = \mathcal{I}^{SZ}(\hat{\sigma} \circ F^m)$  and  $\hat{u}_I \circ F^m = \mathcal{I}^{SZ}(\hat{u} \circ F^m)$ , where  $\mathcal{I}^{SZ}$  is the Scott-Zhang interpolation operator [47] on  $\Omega^1$ . It follows from the same argument in [20, Theorem 4.7.3] that:

$$\|\hat{\sigma} - \hat{\sigma}_I\|_{H(\text{div}, \Omega^m)} + \|\hat{u} - \hat{u}_I\|_{0, \Omega^m} \lesssim h^q (\|\hat{\sigma}\|_{q+1, \Omega^m} + \|\hat{u}\|_{q, \Omega^m}), \quad (67)$$

with  $q = \min\{k, s-1\}$ . Subtracting  $\mathbb{A}^m(\hat{\sigma}_I, \hat{u}_I; \hat{\tau}_h, \hat{v}_h)$  from (66), we can get:

$$\mathbb{A}^m(\hat{\sigma}_h - \hat{\sigma}_I, \hat{u}_h - \hat{u}_I; \hat{\tau}_h, \hat{v}_h) = \mathbb{A}^m(\hat{\sigma} - \hat{\sigma}_I, \hat{u} - \hat{u}_I; \hat{\tau}_h, \hat{v}_h) - E(\hat{\tau}_h, \hat{v}_h). \quad (68)$$

This, combined with the stability result (59) and the geometric error estimate (62), yields

$$\begin{aligned} & \|\hat{\sigma}_h - \hat{\sigma}_I\|_{H(\text{div}, \Omega^m)} + \|\hat{u}_h - \hat{u}_I\|_{0, \Omega} \\ & \lesssim \|\hat{\sigma} - \hat{\sigma}_I\|_{H(\text{div}, \Omega^m)} + \|\hat{u} - \hat{u}_I\|_{0, \Omega^m} + h^{m+\frac{1}{2}} \|u\|_{H^{\frac{5}{2}}(\Omega)}. \end{aligned} \quad (69)$$

The final error estimate (65) follows from the triangle inequality and the interpolation error (67), which completes the proof.

### 5.3 The $L^2$ norm error of stress

The lack of space inclusion  $\text{div } \Sigma_h^m \not\subseteq V_h^m$  makes it difficult to analyze the  $L^2$ -error of stress. The key ingredient here is to prove that the monolithic bilinear form  $\mathbb{A}^m(\cdot, \cdot; \cdot, \cdot)$  is stable on  $\Sigma_h^m \times V_h^m$  in the mesh-dependent norms (70), where the case for  $m = 1$  has been proved in [23, Lemma 3.3]. Moreover, the superclose property of  $u$  has been established.

#### 5.3.1 Stability in mesh-dependent norms

For any  $\tau_h \in \Sigma_h^m$  and  $v_h \in V_h^m$ , denote the mesh-dependent norms:

$$\begin{aligned} \|\tau_h\|_{0,h,m}^2 &:= \|\tau_h\|_{0,\Omega^m}^2 + \sum_{E \in \mathcal{E}_h^m} h_E \|\tau_h \nu_E\|_{0,E}^2, \\ |v_h|_{1,h,m}^2 &:= \|\varepsilon_h(v_h)\|_{0,\Omega^m}^2 + \sum_{E \in \mathcal{E}_h^m} h_E^{-1} \|[[v_h]]\|_{0,E}^2. \end{aligned} \quad (70)$$

Here  $\varepsilon_h$  is the element-wise symmetric gradient and  $[[\cdot]]$  is defined in (9). The following inf-sup condition is important to establish the stability of  $\mathbb{A}^m(\cdot, \cdot; \cdot, \cdot)$ : for  $k \geq 3$ ,

$$|v_h|_{1,h,m} \lesssim \sup_{0 \neq \tau_h \in \Sigma_h^m} \frac{b^m(\tau_h, v_h)}{\|\tau_h\|_{0,h,m}}, \quad \text{for all } v_h \in V_h^m. \quad (71)$$

While the case  $m = 1$  was established in [23, Lemma 3.3], this paper addresses  $m > 1$ . Before proving it, we need the following result which can be obtained by combining [23, (3.6), (3.8)].

$$\|\nabla_h v\|_{0,\Omega^1}^2 + \|v\|_{0,\Omega^1}^2 \lesssim |v|_{1,h,1}^2, \quad \text{for all } v \in H^1(\mathcal{T}_h^1; \mathbb{R}^2). \quad (72)$$

**Lemma 6** *Assume  $k \geq 3$  and  $h$  small enough, the inf-sup condition holds:*

$$|v_h|_{1,h,m} \lesssim \sup_{0 \neq \tau_h \in \Sigma_h^m} \frac{b^m(\tau_h, v_h)}{\|\tau_h\|_{0,h,m}}, \quad \text{for all } v_h \in V_h^m. \quad (73)$$

*Proof* The case  $m = 1$  has been established in [23, Lemma 3.3]. To extend this result to general  $m$ , we require the following three estimates:

$$\|\tau_h\|_{0,h,m} \approx \|\hat{\tau}_h\|_{0,h,1}, \quad |v_h|_{1,h,m} \approx |\hat{v}_h|_{1,h,1}, \quad (74)$$

$$b^m(\tau_h, v_h) \geq b^1(\hat{\tau}_h, \hat{v}_h) - Ch\|\tau_h\|_{0,h,m}|v_h|_{1,h,m}, \quad (75)$$

with  $\hat{\tau}_h = \tau_h \circ \Phi^{lm}$ ,  $\hat{v}_h = v_h \circ \Phi^{lm}$  for  $l = 1$ . Let  $J = \hat{\nabla} \Phi^{lm}$  defined by element-wise. On each element:

$$\|\tau_h\|_{0,K^m}^2 - \|\hat{\tau}_h\|_{0,K^l}^2 = (|\hat{\tau}_h|^2, \det(J) - 1)_{K^l}, \quad (76)$$

$$\begin{aligned} h_{E^m} \|\tau_h \nu_{E^m}\|_{0,E^m}^2 - h_{E^l} \|\hat{\tau}_h \nu_{E^l}\|_{0,E^l}^2 &= (h_{E^m} - h_{E^l}) \|\hat{\tau}_h \nu_{E^l}\|_{0,E^l}^2 \\ &+ h_{E^m} (|\hat{\tau}_h \nu_{E^l}|^2, |J^{-T} \nu_{E^l}|^{-1} \det(J) - 1)_{E^l} \\ &+ h_{E^m} (|\hat{\tau}_h J^{-T} \nu_{E^l}|^2 - |\hat{\tau}_h \nu_{E^l}|^2, |J^{-T} \nu_{E^l}|^{-1} \det(J))_{E^l}. \end{aligned} \quad (77)$$

Utilizing the estimate  $\|J - I\|_{L^\infty(K^l)} \lesssim h^l$  from (22), we bound each term:

$$|\|\tau_h\|_{0,h,m}^2 - \|\hat{\tau}_h\|_{0,h,l}^2| \lesssim h^l \|\hat{\tau}_h\|_{0,h,l}^2. \quad (78)$$

This establishes the first equation in (74). Combining this approach with the discrete Sobolev inequality (72), we further derive the second equation in (74). The inequality (75) follows from the estimate of  $b(\cdot, \cdot)$  in (35), trace theorems [20, Theorem 1.6.6], inverse estimates [20, Lemma 4.5.3], and (72).

*Remark 3* From (23) and the second equation in (74), it follows that (72) also holds over  $\Omega^m$ :

$$\|\nabla_h v\|_{0,\Omega^m}^2 + \|v\|_{0,\Omega^m}^2 \lesssim |v|_{1,h,m}^2, \quad \text{for all } v \in H^1(\mathcal{T}_h^m; \mathbb{R}^2). \quad (79)$$

By the uniform boundedness of  $\mathcal{A}$ , the bilinear form  $a^m(\cdot, \cdot)$  is coercive over the full discrete space:

$$a^m(\sigma_h, \sigma_h) \gtrsim \|\sigma_h\|_{0,h,m}^2, \quad \text{for all } \sigma_h \in \Sigma_h^m. \quad (80)$$

Combining this coercivity with the discrete inf-sup condition (73), we obtain the important stability result.

**Theorem 5** *For  $k \geq 3$  and  $h$  small enough, it follows that for any  $(\sigma_h, u_h) \in \Sigma_h^m \times V_h^m$ ,*

$$\|\sigma_h\|_{0,h,m} + |u_h|_{1,h,m} \lesssim \sup_{(\tau_h, v_h) \in \Sigma_h^m \times V_h^m} \frac{\mathbb{A}^m(\sigma_h, u_h; \tau_h, v_h)}{\|\tau_h\|_{0,h,m} + |v_h|_{1,h,m}}. \quad (81)$$



### 5.3.2 Error estimate

The following lemma estimates the consistency error arising from the non-inclusion, i.e.,  $\operatorname{div} \Sigma_h^m \not\subseteq V_h^m$ . This results in a half-order reduction in the convergence rate of the stress field compared to the optimal order.

**Lemma 7** *Let  $Q_h : L^2(\Omega^m; \mathbb{R}^2) \rightarrow V_h^m$  denote the  $L^2$ -orthogonal projection operator. For all  $\tau \in \Sigma_h^m$ , the following consistency error estimate holds,*

$$|b^m(\tau, (I - Q_h)u)| \lesssim \min \{h|\tau|_{1, \mathcal{T}_{\partial, h}^m}, \|\tau\|_{0, \Omega_S^m}\} \|(I - Q_h)u\|_{0, \Omega_S^m}. \quad (82)$$

Moreover, if  $u \in H^{s+1}(\Omega^m; \mathbb{R}^2)$ ,

$$|b^m(\tau, (I - Q_h)u)| \lesssim \min \{h^{q+1}|\tau|_{1, \mathcal{T}_{\partial, h}^m}, h^q\|\tau\|_{0, \Omega_S^m}\} \|u\|_{H^q(\Omega^m)}, \quad (83)$$

where  $q = \min\{k + \frac{1}{2}, s + 1\}$ , and  $|\tau|_{1, \mathcal{T}_{\partial, h}^m} = (\sum_{K^m \in \mathcal{T}_{\partial, h}^m} |\tau|_{1, K^m}^2)^{\frac{1}{2}}$ .

*Proof* By the projection property of  $Q_h$  and  $(I - Q_h) \operatorname{div} \tau = 0$  on all interior elements, we derive

$$b^m(\tau, (I - Q_h)u) = \sum_{K^m \in \mathcal{T}_{\partial, h}^m} ((I - Q_h) \operatorname{div} \tau, (I - Q_h)u)_{K^m}. \quad (84)$$

Applying the Cauchy-Schwarz inequality and the estimate of  $\tau$  in Lemma 2, we establish (82). Furthermore, (83) stems from the error estimate:  $\|(I - Q_h)u\|_{0, K^m} \lesssim h^q |u|_{H^q(K^m)}$  with  $q = \min\{k, s + 1\}$  and (60).

Before presenting the final error estimate, we define a global interpolation operator  $\Pi_h : H^1(\Omega^m; \mathbb{S}) \rightarrow \Sigma_h^m$ . Let  $\Pi_h^1 : H^1(\Omega^1; \mathbb{S}) \rightarrow \Sigma_h^1$  denote the standard interpolation operator as defined in [33, Remark 3.1], which satisfies

$$b^1(\tau - \Pi_h^1 \tau, v_h) = 0, \quad \text{for all } \tau \in H^1(\Omega^1; \mathbb{S}), v_h \in V_h^1. \quad (85)$$

For each  $K^1 \in \mathcal{T}_h^1$ , recall the mapping  $\Phi_K^{1m} : K^1 \rightarrow K^m \in \mathcal{T}_h^m$ . Then, for any  $\tau \in \Sigma_h^m$ , the operator  $\Pi_h$  is defined element-wise by

$$\Pi_h \tau|_{K^m} = (\Pi_h^1 \hat{\tau}|_{K^1}) \circ (\Phi_K^{1m})^{-1}, \quad (86)$$

where  $\hat{\tau} := \tau \circ \Phi_K^{1m}$ . Although  $\Pi_h$  does not satisfy a commutative property analogous to (85), it follows from (35) with  $l = 1$  that

$$|b^m(\tau - \Pi_h \tau, v_h)| \lesssim h \|\tau - \Pi_h \tau\|_{0, h, m} |v_h|_{1, h, m} \quad (87)$$

for all  $\tau \in H^1(\Omega^m; \mathbb{S})$  and  $v_h \in V_h^m$ . If  $\tau \in H^s(\Omega^m; \mathbb{S})$  with  $1 \leq s \leq k + 1$ , using the techniques in [20, Section 4.4], we have the following interpolation error estimate

$$\|\tau - \Pi_h \tau\|_{0, h, m} + h \|\tau - \Pi_h \tau\|_{1, \mathcal{T}_h^m} \lesssim h^s \|\tau\|_{s, \Omega^m}. \quad (88)$$

**Theorem 6** *Under the hypotheses of Lemma 5 and Theorem 4, the following error estimate holds,*

$$\|\hat{\sigma} - \hat{\sigma}_h\|_{0,h,m} + |Q_h \hat{u} - \hat{u}_h|_{1,h,m} \lesssim h^{\min\{k+\frac{1}{2}, m+\frac{1}{2}, s\}} \|u\|_{H^{s+1}(\Omega)}. \quad (89)$$

Moreover, if  $\Omega^m$  is convex,

$$\|Q_h \hat{u} - \hat{u}_h\|_{0,\Omega^m} \lesssim h^{\min\{k+\frac{3}{2}, m+1, s+1\}} \|u\|_{H^{s+1}(\Omega)}, \quad (90)$$

$$\|\hat{u} - \hat{u}_h\|_{0,\Omega^m} \lesssim h^{\min\{k, m+1, s+1\}} \|u\|_{H^{s+1}(\Omega)}. \quad (91)$$

*Proof* By subtracting  $\mathbb{A}^m(\Pi_h \hat{\sigma}, Q_h \hat{u}; \hat{\tau}_h, \hat{v}_h)$  from both sides of (66) and using the definition of  $\mathbb{A}^m$ , we obtain

$$\begin{aligned} & \mathbb{A}^m(\Pi_h \hat{\sigma} - \hat{\sigma}_h, Q_h \hat{u} - \hat{u}_h; \hat{\tau}_h, \hat{v}_h) \\ &= a^m(\Pi_h \hat{\sigma} - \hat{\sigma}_h, \hat{\tau}_h) + b^m(\Pi_h \hat{\sigma} - \hat{\sigma}_h, \hat{v}_h) + b^m(\hat{\tau}_h, Q_h \hat{u} - \hat{u}) + E(\hat{\tau}_h, \hat{v}_h). \end{aligned} \quad (92)$$

The combination of (62) and (79) implies

$$|E(\hat{\tau}, \hat{v})| \leq Ch^{m+\frac{1}{2}} (\|\hat{\tau}\|_{0,h,m} + |\hat{v}|_{1,h,m}) \|u\|_{H^{\frac{5}{2}}(\Omega)}. \quad (93)$$

This estimate, together with (92), the stability result of  $\mathbb{A}^m(\cdot, \cdot; \cdot, \cdot)$  in (81), the bound on  $b^m(\hat{\sigma} - \Pi_h \hat{\sigma}, \hat{v}_h)$  in (87), and the estimate of  $b^m(\hat{\tau}_h, (I - Q_h)\hat{u})$  in (83), yields

$$\|\Pi_h \hat{\sigma} - \hat{\sigma}_h\|_{0,h,m} + |Q_h \hat{u} - \hat{u}_h|_{1,h,m} \lesssim \|\Pi_h \hat{\sigma} - \hat{\sigma}_h\|_{0,h,m} + h^q \|u\|_{H^{s+1}(\Omega)}, \quad (94)$$

where  $q = \min\{k + \frac{1}{2}, m + \frac{1}{2}, s + 1\}$ . Finally, applying inequality (94) along with the interpolation error estimate of  $\Pi_h$  in (88) leads to the desired bound (89).

The error estimate (90) can be derived by using the duality argument following [28, 54]. Consider the dual problem: find  $(z, w) \in H(\text{div}, \Omega^m; \mathbb{S}) \times L^2(\Omega^m; \mathbb{R}^2)$ , such that

$$\begin{cases} a^m(\tau, z) + b^m(\tau, w) = 0, & \text{for all } \tau \in H(\text{div}, \Omega^m; \mathbb{S}), \\ b^m(z, v) = (Q_h \hat{u} - \hat{u}_h, v), & \text{for all } v \in L^2(\Omega^m; \mathbb{R}^2). \end{cases} \quad (95)$$

Due to the convexity of  $\Omega^m$ , the solutions admit the regularity:

$$\|z\|_{1,\Omega^m} + \|w\|_{2,\Omega^m} \lesssim \|Q_h \hat{u} - \hat{u}_h\|_{0,\Omega^m}. \quad (96)$$

Let  $(z_h, w_h) \in \Sigma_h^m \times V_h^m$  such that  $z_h = \Pi_h z$  and  $w_h = Q_h w$ . Selecting test functions  $v = Q_h \hat{u} - \hat{u}_h$  and  $\tau = \hat{\sigma} - \hat{\sigma}_h$  in (95), we obtain:

$$\begin{aligned} \|Q_h \hat{u} - \hat{u}_h\|_{0,\Omega^m}^2 &= a^m(\hat{\sigma} - \hat{\sigma}_h, z - z_h) + b^m(\hat{\sigma} - \hat{\sigma}_h, w - w_h) \\ &\quad + E(z_h, w_h) + b^m(z - z_h, Q_h \hat{u} - \hat{u}_h) - b^m(z_h, \hat{u} - Q_h \hat{u}). \end{aligned} \quad (97)$$

It follows from the quasi-commutative property (87) and the superclose result (89) that

$$|b^m(z - z_h, Q_h \hat{u} - \hat{u}_h)| \lesssim h^{q+1} \|z - \Pi_h z\|_{0,h,m} \|u\|_{H^{s+1}(\Omega)}, \quad (98)$$

with  $q = \min\{k + \frac{1}{2}, m + \frac{1}{2}, s\}$ . Combining this with (88) and (96), we obtain

$$|b^m(z - z_h, Q_h \hat{u} - \hat{u}_h)| \lesssim h^{\min\{k+\frac{5}{2}, m+\frac{5}{2}, s+2\}} \|Q_h \hat{u} - \hat{u}_h\|_{0, \Omega^m} \|u\|_{H^{s+1}(\Omega)}. \quad (99)$$

The definition of  $z_h$  and the interpolation error (88) imply

$$\|z_h\|_{1, \mathcal{T}_h^m} \leq \|z\|_{1, \Omega^m} + \|\Pi_h z - z\|_{1, \mathcal{T}_h^m} \lesssim \|z\|_{1, \Omega^m}. \quad (100)$$

This, together with (96) and the estimate of  $b^m(z_h, \hat{u} - Q_h \hat{u})$  in (83), yields

$$|b^m(z_h, \hat{u} - Q_h \hat{u})| \lesssim h^{\min\{k+\frac{3}{2}, s+2\}} \|Q_h \hat{u} - \hat{u}_h\|_{0, \Omega^m} \|u\|_{H^{s+1}(\Omega)}. \quad (101)$$

Applying the triangle inequality, (60) and (88), we derive:  $\|z_h\|_{0, \Omega_S^m} \leq \|z_h - z\|_{0, \Omega^m} + \|z\|_{0, \Omega_S^m} \lesssim (1 + h^{\frac{1}{2}}) h^{\frac{1}{2}} \|z\|_{1, \Omega^m}$ . This result, combined with an analogous argument for  $\|w_h\|_{0, \Omega_S^m}$ , the estimate of  $|E(z_h, w_h)|$  in (62), and (96), leads to:

$$|E(z_h, w_h)| \lesssim h^{m+1} \|Q_h \hat{u} - \hat{u}_h\|_{0, \Omega^m} \|u\|_{H^{\frac{5}{2}}(\Omega)}. \quad (102)$$

Integrating the error estimates of  $\hat{\sigma} - \hat{\sigma}_h$  in (65) and (89), we derive:

$$|a^m(\hat{\sigma} - \hat{\sigma}_h, z - z_h)| \lesssim h^{\min\{m+\frac{3}{2}, k+\frac{3}{2}, s+1\}} \|u\|_{s+1, \Omega} \|Q_h \hat{u} - \hat{u}_h\|_{0, \Omega^m}, \quad (103)$$

$$|b^m(\hat{\sigma} - \hat{\sigma}_h, w - w_h)| \lesssim h^{\min\{m+\frac{5}{2}, k+2, s+1\}} \|u\|_{s+1, \Omega} \|Q_h \hat{u} - \hat{u}_h\|_{0, \Omega^m}. \quad (104)$$

Combining (97), (103), (104), (102), (101) and (99), we obtain the superclose result (90). The error estimate (91) follows from the triangle inequality and the approximation property of  $Q_h$ , which completes the proof.

*Remark 4* For sufficiently large  $m, s$  (specifically,  $m, s \geq k + 1$ ),

$$\|\hat{\sigma} - \hat{\sigma}_h\|_{0, \Omega^m} = \mathcal{O}(h^{k+\frac{1}{2}}). \quad (105)$$

The result exhibits a convergence rate that is half an order lower than the optimal rate of  $k + 1$ . As shown in our analysis, this degradation arises from the consistency error introduced by curved boundary elements. To remedy this issue, we introduce the following enriched finite element spaces. First we define the enriched spaces on  $\Omega^1$ ,

$$\begin{aligned} \widetilde{\Sigma}_h^1 &:= \{\sigma_h \in H(\operatorname{div}, \Omega^1; \mathbb{S}) : \sigma_h = \sigma_c + \sigma_b, \sigma_c \in H^1(\Omega^1; \mathbb{S}), \\ &\quad \sigma_c|_{K^1} \in P_k(K^1; \mathbb{S}), \sigma_b|_{K^1} \in \Sigma_{k,b}(K^1), \text{ for all } K^1 \in \mathcal{T}_{i,h}^1, \\ &\quad \sigma_c|_{K^1} \in P_{k+1}(K^1; \mathbb{S}), \sigma_b|_{K^1} \in \Sigma_{k+1,b}(K^1), \text{ for all } K^1 \in \mathcal{T}_{\partial,h}^1\}, \end{aligned} \quad (106)$$

$$\begin{aligned} \widetilde{V}_h^1 &:= \{v_h \in L^2(\Omega^1; \mathbb{R}^2) : v_h|_{K^1} \in P_{k-1}(K^1, \mathbb{R}^2), \text{ for all } K^1 \in \mathcal{T}_{i,h}^1, \\ &\quad v_h|_{K^1} \in P_k(K^1, \mathbb{R}^2), \text{ for all } K^1 \in \mathcal{T}_{\partial,h}^1\}, \end{aligned} \quad (107)$$

recall that  $\mathcal{T}_{i,h}^1, \mathcal{T}_{\partial,h}^1$  are the sets of inner and boundary triangles, respectively. Then the enriched spaces  $\widetilde{\Sigma}_h^m, \widetilde{V}_h^m$  over  $\Omega^m$  can be defined in the same way as in (26).

Solving the discrete problem (32) with the enriched spaces  $\widetilde{\Sigma}_h^m$  and  $\widetilde{V}_h^m$ , the  $L^2$ -error estimate for  $\sigma$  is recovered to the optimal order  $k + 1$ . It is worth noting that this modification is limited to the boundary elements and incurs only a marginal increase in the number of degrees of freedom.

*Remark 5* The postprocessing of the displacement field is a common practice in mixed-method analyses: find  $\hat{u}_h^* \in V_h^{m,*}$  and  $\hat{\phi}_h \in V_h^m$ , such that for all  $K^m \in \mathcal{T}_h^m$ ,  $v \in V_h^{m,*}|_{K^m}$  and  $\psi \in V_h^m|_{K^m}$ , satisfying

$$\begin{cases} (\varepsilon(\hat{u}_h^*), \varepsilon(v))_{K^m} + (v, \hat{\phi}_h)_{K^m} = (\mathcal{A}\hat{\sigma}_h, \varepsilon(v))_{K^m}, \\ (\hat{u}_h^*, \psi)_{K^m} = (\hat{u}_h, \psi)_{K^m}. \end{cases} \quad (108)$$

Where the space  $V_h^{m,*}$  is defined as

$$V_h^{m,*} := \{v \in L^2(\Omega^m; \mathbb{R}^2) : v|_{K^m} \circ F_K^m \in P_{k+1}(K^1; \mathbb{R}^2), \text{ for all } K^1 \in \mathcal{T}_h^1\}. \quad (109)$$

Following the proof in [23] and (90), we can get

$$\|\hat{u} - \hat{u}_h^*\|_{0,\Omega^m} \lesssim h^{\min\{k+\frac{3}{2}, m+1, s+1\}} \|u\|_{H^{s+1}(\Omega)}. \quad (110)$$

*Remark 6* The above theory can be extended to the inhomogeneous case with the displacement boundary condition  $u|_\Gamma = g_D \in H^{\frac{1}{2}}(\Gamma)$ . Construct a  $u_D \in H^1(\Omega)$  such that  $u_D = g_D$  on  $\Gamma$ . The first equation in (1) is replaced by

$$a(\sigma, \tau) + b(\tau, \hat{u}) = -b(\tau, u_D) + (g_D, \tau \cdot n)_\Gamma, \quad \text{for all } \tau \in \Sigma, \quad (111)$$

where  $\hat{u} = u - u_D$ . The right-hand-side of (111) is just  $(\tau, \nabla u_D)$ , which contains no boundary term. The discrete problem is to find  $(\sigma_h, \hat{u}_h) \in \Sigma_h^m \times V_h^m$  such that

$$\begin{cases} a^m(\sigma_h, \tau_h) + b^m(\tau_h, \hat{u}_h) = (\tau_h, \widetilde{\nabla u_D})_{\Omega^m}, & \text{for all } \tau_h \in \Sigma_h^m, \\ b^m(\sigma_h, v_h) = -(f, v_h)_{\Omega^m} & \text{for all } v_h \in V_h^m, \end{cases} \quad (112)$$

here  $\tilde{g} := g \circ \Psi^m \det(\nabla \Psi^m)$  with  $g = \nabla u_D$  or  $g = f$ . Discrete displacement can be taken as  $\hat{u}_h = \hat{u}_h + Q_h u_D$ . Then the geometric error in (61) is redefined as

$$\mathcal{A}^m(\hat{\sigma}, \hat{u}; \hat{\tau}, \hat{v}) = (\tau, \nabla u_D)_\Omega - (f, v)_\Omega + E(\hat{\tau}, \hat{v}), \quad (113)$$

and the proof for the error analysis proceeds in essentially the same manner as in the preceding argument.

*Remark 7* As in [23, 38], our algorithm and analysis can be extended to nearly incompressible or incompressible elastic materials. For example, in the homogeneous isotropic case, the coercivity constant of the compliance tensor  $\mathcal{A}$  is independent of the Lamé constant  $\lambda$ , which stems from [17, Proposition 9.1.1].

## 6 Numerical results

This section presents the competitive relationship between polynomial degree  $k$  and geometric approximation order  $m$  through numerical experiments on both unit disk and an asymmetric domain. All meshes were generated by Gmsh (version 4.13.1, <http://gmsh.info>, [29]) with a successive uniform refinement scheme. Errors including  $\|\hat{u} - \hat{u}_h\|_{L^2(\Omega^m)}$ ,  $\|\hat{u} - \hat{u}_h^*\|_{L^2(\Omega^m)}$ ,  $\|\hat{\sigma} - \hat{\sigma}_h\|_{L^2(\Omega^m)}$  and  $\|\hat{\text{div}} \hat{\sigma} - \hat{\text{div}} \hat{\sigma}_h\|_{L^2(\Omega^m)}$  were calculated over the discrete domain  $\Omega^m$ . All computation was done with MATLAB, where we used the “backslash” command in MATLAB to solve the linear systems.

### 6.1 Unit disk domain

We test our results over the unit disk  $\Omega = \{(x, y) : x^2 + y^2 \leq 1\}$ . The exact solution is taken as

$$u(x, y) = (e^{xy} \cos(x) e^y \sin(x + y))^T, \quad (114)$$

and the Lamé constants are taken as  $\lambda = 1, \mu = 1$ .

First, we perform the computation using the spaces  $\Sigma_h^m$  and  $V_h^m$ . Table 1 reports the estimated orders of convergence (EoC), computed as the slopes of linear regressions over the last three mesh levels in a sequence of uniformly refined meshes. As expected,  $L^2$  and  $H(\text{div})$  errors of the stress are consistent with theoretical predictions. Specifically, the convergence rate of  $L^2$  errors of  $\hat{\sigma}_h$  is  $\min\{k + \frac{1}{2}, m + \frac{1}{2}\}$ , which does not attain the optimal order  $k + 1$  even when  $m > k$ . For  $\hat{\text{div}}\hat{\sigma}_h$ , the observed rate is  $\min\{k, m + \frac{1}{2}\}$ . When  $m$  is odd, the  $L^2$  errors of both the displacement and its post-processed version align well with the theoretical expectations, which are  $\min\{k, m + 1\}$  and  $\min\{k + \frac{3}{2}, m + 1\}$ , respectively. In contrast, for even values of  $m$ , the  $L^2$  error orders for both quantities appear to exceed the theoretical rates by approximately half an order, though this has limited practical impact.

The right half of Table 1 presents results obtained using the modified spaces  $\widetilde{\Sigma}_h^m$  and  $\widetilde{V}_h^m$ . The primary improvement brought by this modification is that the EoC for  $\|\hat{u} - \hat{u}_h^*\|_{L^2}$  and  $\|\hat{\sigma} - \hat{\sigma}_h\|_{L^2}$  increase by half an order for  $m = k + 1$ , in full agreement with theoretical predictions.

**Table 1** EoC for unit disk.  $N_T$  is the number of elements in the final mesh.  $m$  and  $k$  are the order of mesh and finite element spaces respectively.

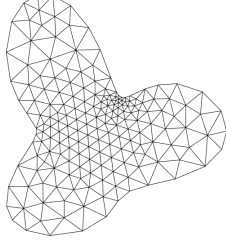
$N_T$	$k$	$m$	$\Sigma_h^m \times V_h^m$				$\widetilde{\Sigma}_h^m \times \widetilde{V}_h^m$			
			$\hat{u}$	$\hat{u}_h^*$	$\hat{\sigma}_h$	$\hat{\text{div}}\hat{\sigma}_h$	$\hat{u}$	$\hat{u}_h^*$	$\hat{\sigma}_h$	$\hat{\text{div}}\hat{\sigma}_h$
14336	3	1	1.97	1.98	1.54	1.51	2.05	2.05	1.58	1.51
	3	2	3.04	3.50	2.50	2.50	2.96	3.53	2.50	2.52
	3	3	3.03	4.41	3.51	3.14	2.93	4.09	3.57	2.94
	3	4	3.03	4.49	3.51	3.14	2.93	4.97	3.97	2.93
14336	4	1	1.98	1.98	1.52	1.51	2.05	2.05	1.58	1.51
	4	2	3.50	3.50	2.50	2.49	3.54	3.54	2.50	2.49
	4	3	4.09	4.00	3.51	3.53	3.97	4.08	3.52	3.55
	4	4	4.09	5.50	4.49	4.17	3.94	5.68	4.68	3.89
	4	5	4.09	5.49	4.49	4.18	3.94	5.89	4.88	3.88

### 6.2 Three leaf boundary domain

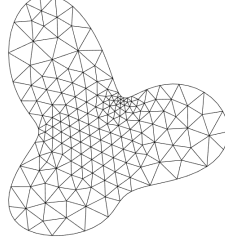
As in [8], we test on the  $\Omega$  whose boundary is parametrized by

$$\begin{cases} x(t) = [1 + 0.4 \cos(3t)] \cos(t), \\ y(t) = [1 + (0.4 + 0.22 \sin(t)) \cos(3t)] \sin(t), \end{cases} \quad (115)$$

where  $0 \leq t \leq 2\pi$ . The coarsest mesh is shown in Figure 1. It is evident that the domain is non-convex. To generate a regular mesh, we deliberately applied local refinement near the concave corners in advance. The exact solution is taken the same as (114). As indicated in Table 2, most results align with those



(a)  $m = 1$ ,  $N_T = 332$ .



(b)  $m = 3$ ,  $N_T = 332$ .

**Fig. 1** Illustration of the three-leaf domain with mesh order  $m = 1$  (left) and  $m = 3$  (right).

from the first numerical example and closely match the theoretical predictions. Minor deviations observed in a few cases may be due to the non-convexity of the domain. Nevertheless, the method remains capable of producing reasonably accurate results even on certain non-convex geometries.

**Table 2** EoC for three-leaf domain.  $N_T$  is the number of elements in the final mesh.  $m$  and  $k$  are the order of mesh and finite element spaces respectively.

$N_T$	$k$	$m$	$\Sigma_h^m \times V_h^m$				$\widetilde{\Sigma}_h^m \times \widetilde{V}_h^m$			
			$\hat{u}$	$\hat{u}_h^*$	$\hat{\sigma}_h$	$\hat{\text{div}}\hat{\sigma}_h$	$\hat{u}$	$\hat{u}_h^*$	$\hat{\sigma}_h$	$\hat{\text{div}}\hat{\sigma}_h$
84992	3	1	1.98	1.98	1.54	1.51	2.04	2.05	1.59	1.51
	3	2	3.18	3.52	2.50	2.49	3.15	3.55	2.49	2.50
	3	3	3.13	4.16	3.53	3.31	2.89	4.08	3.53	3.09
	3	4	3.13	4.48	3.52	3.32	2.89	5.15	4.14	2.95
21248	4	1	1.96	1.96	1.56	1.51	1.97	1.97	1.61	1.51
	4	2	3.52	3.52	2.49	2.49	3.54	3.54	2.49	2.49
	4	3	4.20	4.02	3.50	3.49	4.00	4.01	3.52	3.47
	4	4	4.41	5.46	4.48	4.23	3.90	5.53	4.48	4.20
	4	5	4.41	5.46	4.47	4.22	3.86	5.99	5.17	4.16

**Acknowledgements** The first and second authors would like to thank Professor Rui Ma from Beijing Institute of Technology for her valuable suggestions on the proof of the inf-sup condition in this article.

## References

1. Adams, S., Cockburn, B.: A mixed finite element method for elasticity in three dimensions. *J. Sci. Comput.* **25**(3), 515–521 (2005)
2. Amara, M., Thomas, J.M.: Equilibrium finite elements for the linear elastic problem. *Numer. Math.* **33**(4), 367–383 (1979)
3. Arnold, D.N., Awanou, G.: Rectangular mixed finite elements for elasticity. *Math. Models Methods Appl. Sci.* **15**(9), 1417–1429 (2005)
4. Arnold, D.N., Awanou, G., Winther, R.: Finite elements for symmetric tensors in three dimensions. *Math. Comp.* **77**(263), 1229–1251 (2008)
5. Arnold, D.N., Brezzi, F., Douglas Jr., J.: PEERS: a new mixed finite element for plane elasticity. *Japan J. Appl. Math.* **1**(2), 347–367 (1984)
6. Arnold, D.N., Douglas Jr., J., Gupta, C.P.: A family of higher order mixed finite element methods for plane elasticity. *Numer. Math.* **45**(1), 1–22 (1984)
7. Arnold, D.N., Falk, R.S., Winther, R.: Mixed finite element methods for linear elasticity with weakly imposed symmetry. *Math. Comp.* **76**(260), 1699–1723 (2007)
8. Arnold, D.N., Walker, S.W.: The Hellan-Herrmann-Johnson method with curved elements. *SIAM J. Numer. Anal.* **58**(5), 2829–2855 (2020)
9. Arnold, D.N., Winther, R.: Mixed finite elements for elasticity. *Numer. Math.* **92**(3), 401–419 (2002)
10. Arnold, D.N., Winther, R.: Nonconforming mixed elements for elasticity. *Math. Models Methods Appl. Sci.* **13**(3), 295–307 (2003)
11. Awanou, G.: Two remarks on rectangular mixed finite elements for elasticity. *J. Sci. Comput.* **50**(1), 91–102 (2012)
12. Bae, H.O., Kim, D.W.: Finite element approximations for the Stokes equations on curved domains, and their errors. *Appl. Math. Comput.* **148**(3), 823–847 (2004)
13. Bernardi, C.: Optimal finite-element interpolation on curved domains. *SIAM J. Numer. Anal.* **26**(5), 1212–1240 (1989)
14. Bertrand, F., Münzenmaier, S., Starke, G.: First-order system least squares on curved boundaries: higher-order Raviart-Thomas elements. *SIAM J. Numer. Anal.* **52**(6), 3165–3180 (2014)
15. Bertrand, F., Starke, G.: Parametric Raviart-Thomas elements for mixed methods on domains with curved surfaces. *SIAM J. Numer. Anal.* **54**(6), 3648–3667 (2016)
16. Boffi, D., Brezzi, F., Fortin, M.: Reduced symmetry elements in linear elasticity. *Commun. Pure Appl. Anal.* **8**(1), 95–121 (2009)
17. Boffi, D., Brezzi, F., Fortin, M.: Mixed finite element methods and applications, *Springer Series in Computational Mathematics*, vol. 44. Springer, Heidelberg (2013)
18. Brandts, J.H.: Superconvergence and a posteriori error estimation for triangular mixed finite elements. *Numer. Math.* **68**(3), 311–324 (1994)
19. Brenner, S.C., Neilan, M., Sung, L.Y.: Isoparametric  $C^0$  interior penalty methods for plate bending problems on smooth domains. *Calcolo* **50**(1), 35–67 (2013)
20. Brenner, S.C., Scott, L.R.: The mathematical theory of finite element methods, *Texts in Applied Mathematics*, vol. 15, third edn. Springer, New York (2008)
21. Caubet, F., Ghanous, J., Pierre, C.: A priori error estimates of a Poisson equation with Ventcel boundary conditions on curved meshes. *SIAM J. Numer. Anal.* **62**(4), 1929–1955 (2024)
22. Chen, L., Hu, J., Huang, X.: Stabilized mixed finite element methods for linear elasticity on simplicial grids in  $\mathbb{R}^n$ . *Comput. Methods Appl. Math.* **17**(1), 17–31 (2017)
23. Chen, L., Hu, J., Huang, X.: Fast auxiliary space preconditioners for linear elasticity in mixed form. *Math. Comp.* **87**(312), 1601–1633 (2018)
24. Chen, S.C., Wang, Y.N.: Conforming rectangular mixed finite elements for elasticity. *J. Sci. Comput.* **47**(1), 93–108 (2011)
25. Ciarlet, P.G., Raviart, P.A.: Interpolation theory over curved elements, with applications to finite element methods. *Comput. Methods Appl. Mech. Engrg.* **1**, 217–249 (1972)
26. Cockburn, B., Gopalakrishnan, J., Guzmán, J.: A new elasticity element made for enforcing weak stress symmetry. *Math. Comp.* **79**(271), 1331–1349 (2010)
27. Dione, I., Urquiza, J.M.: Penalty: finite element approximation of Stokes equations with slip boundary conditions. *Numer. Math.* **129**(3), 587–610 (2015)

28. Douglas Jr., J., Roberts, J.E.: Global estimates for mixed methods for second order elliptic equations. *Math. Comp.* **44**(169), 39–52 (1985)
29. Geuzaine, C., Remacle, J.F.: Gmsh: A 3-D finite element mesh generator with built-in pre- and post-processing facilities. *Internat. J. Numer. Methods Engrg.* **79**(11), 1309–1331 (2009)
30. Gopalakrishnan, J., Guzmán, J.: Symmetric nonconforming mixed finite elements for linear elasticity. *SIAM J. Numer. Anal.* **49**(4), 1504–1520 (2011)
31. Gopalakrishnan, J., Guzmán, J.: A second elasticity element using the matrix bubble. *IMA J. Numer. Anal.* **32**(1), 352–372 (2012)
32. Guzmán, J.: A unified analysis of several mixed methods for elasticity with weak stress symmetry. *J. Sci. Comput.* **44**(2), 156–169 (2010)
33. Hu, J.: Finite element approximations of symmetric tensors on simplicial grids in  $\mathbb{R}^n$ : the higher order case. *J. Comput. Math.* **33**(3), 283–296 (2015)
34. Hu, J.: A new family of efficient conforming mixed finite elements on both rectangular and cuboid meshes for linear elasticity in the symmetric formulation. *SIAM J. Numer. Anal.* **53**(3), 1438–1463 (2015)
35. Hu, J., Man, H., Zhang, S.: A simple conforming mixed finite element for linear elasticity on rectangular grids in any space dimension. *J. Sci. Comput.* **58**(2), 367–379 (2014)
36. Hu, J., Shi, Z.C.: Lower order rectangular nonconforming mixed finite elements for plane elasticity. *SIAM J. Numer. Anal.* **46**(1), 88–102 (2007)
37. Hu, J., Zhang, S.: A family of conforming mixed finite elements for linear elasticity on triangular grids. *arXiv:1406.7457 [math.NA]* (2014)
38. Hu, J., Zhang, S.: A family of symmetric mixed finite elements for linear elasticity on tetrahedral grids. *Sci. China Math.* **58**(2), 297–307 (2015)
39. Hu, J., Zhang, S.: Finite element approximations of symmetric tensors on simplicial grids in  $\mathbb{R}^n$ : the lower order case. *Math. Models Methods Appl. Sci.* **26**(9), 1649–1669 (2016)
40. Johnson, C., Mercier, B.: Some equilibrium finite element methods for two-dimensional elasticity problems. *Numer. Math.* **30**(1), 103–116 (1978)
41. Lenoir, M.: Optimal isoparametric finite elements and error estimates for domains involving curved boundaries. *SIAM J. Numer. Anal.* **23**(3), 562–580 (1986)
42. Man, H.Y., Hu, J., Shi, Z.C.: Lower order rectangular nonconforming mixed finite element for the three-dimensional elasticity problem. *Math. Models Methods Appl. Sci.* **19**(1), 51–65 (2009)
43. Morley, M.E.: A family of mixed finite elements for linear elasticity. *Numer. Math.* **55**(6), 633–666 (1989)
44. Neilan, M., Otus, B.: Divergence-free Scott-Vogelius elements on curved domains. *SIAM J. Numer. Anal.* **59**(2), 1090–1116 (2021)
45. Qiu, W., Demkowicz, L.: Mixed variable order  $h$ -finite element method for linear elasticity with weakly imposed symmetry. *Curvilinear elements in 2D. Comput. Methods Appl. Math.* **11**(4), 510–539 (2011)
46. Scott, L.R.: Finite element techniques for curved boundaries. Ph.D. Thesis, Massachusetts Institute of Technology (1973)
47. Scott, L.R., Zhang, S.: Finite element interpolation of nonsmooth functions satisfying boundary conditions. *Math. Comp.* **54**(190), 483–493 (1990)
48. Sky, A., Muench, I.: Polytopal templates for semi-continuous vectorial finite elements of arbitrary order on triangulations and tetrahedralizations. *Finite Elem. Anal. Des.* **236**, Paper No. 104155, 28 (2024)
49. Sky, A., Muench, I., Rizzi, G., Neff, P.: Higher order Bernstein-Bézier and Nédélec finite elements for the relaxed micromorphic model. *J. Comput. Appl. Math.* **438**, Paper No. 115568, 32 (2024)
50. Sky, A., Neunteufel, M., Hale, J.S., Zilian, A.: A Reissner-Mindlin plate formulation using symmetric Hu-Zhang elements via polytopal transformations. *Comput. Methods Appl. Mech. Engrg.* **416**, Paper No. 116291, 29 (2023)
51. Song, S., Liu, Z.: A second-order isoparametric element method to solve plane linear elastic problem. *Numer. Methods Partial Differential Equations* **37**(2), 1535–1550 (2021)
52. Stenberg, R.: On the construction of optimal mixed finite element methods for the linear elasticity problem. *Numer. Math.* **48**(4), 447–462 (1986)



- 
53. Stenberg, R.: A family of mixed finite elements for the elasticity problem. *Numer. Math.* **53**(5), 513–538 (1988)
  54. Stenberg, R.: Postprocessing schemes for some mixed finite elements. *RAIRO Modél. Math. Anal. Numér.* **25**(1), 151–167 (1991)
  55. Verfürth, R.: Finite element approximation of incompressible Navier-Stokes equations with slip boundary condition. *Numer. Math.* **50**(6), 697–721 (1987)
  56. Walker, S.W.: The Kirchhoff plate equation on surfaces: the surface Hellan-Herrmann-Johnson method. *IMA J. Numer. Anal.* **42**(4), 3094–3134 (2022)
  57. Yi, S.Y.: Nonconforming mixed finite element methods for linear elasticity using rectangular elements in two and three dimensions. *Calcolo* **42**(2), 115–133 (2005)
  58. Yi, S.Y.: A new nonconforming mixed finite element method for linear elasticity. *Math. Models Methods Appl. Sci.* **16**(7), 979–999 (2006)